Desalination and Water Treatment
www.deswater.com
doi: 10.5004/dwt.2023.30041

314 (2023) 339–351
December

Combining pore structure types and reservoir forming limits to determine the grading evaluation criteria of Chang 7 tight oil reservoirs in Jiyuan Area, Ordos Basin

Jiangshan Li[a], Quanpei Zhang[b,*], Yong Li[b], Yong Huo[b], Chun Li[a], Duoduo Zhang[b], Kun Lin[b], Caiping Yi[b], Yalan Xue[b]

[a]*Wuqi Oil Production Plant, Shaanxi Yanchang Petroleum (Group) Co., Ltd., Wuqi 717600, China*
[b]*Wuhua Energy Technology Co., Ltd., Xi'an 710061, China, email: 846863720@qq.com (Q. Zhang)*

Received 1 December 2022; Accepted 22 September 2023

ABSTRACT

In view of the common problems of difficult in characterizing pore structure, weak research on reservoir forming limit, and ambiguous meaning of grading evaluation boundary in Chang 7 tight oil reservoirs of the Jiyuan area, Ordos Basin. The pore structure types and reservoir forming limits of tight sandstone were determined by high-pressure mercury injection test and other methods, and the grading criteria were established to evaluate the reservoir quality. The results showed that the Chang 7 tight oil reservoirs have poor petrophysical properties and four types of pore structures, which correspond to different reservoir types respectively. There are three types of the reservoir forming limits in tight sandstone reservoirs, namely the theoretical lower limit, lower limit of oil accumulation, and effective seepage lower limit, with the corresponding porosity limits of 3.5%, 5.5%, and 8.0%, respectively, and the corresponding permeability limits of 0.02×10^{-3} μm^2, 0.05×10^{-3} μm^2, and 0.20×10^{-3} μm^2, respectively. These reservoir forming limits were in good agreement with the classification boundaries of pore structure. Combining the pore structure types with the reservoir forming limits, the Chang 7 tight oil reservoirs can be divided into four classes: I, II, III, and IV, representing easily movable tight reservoir, movable tight reservoir, oil-bearing tight reservoir, and ineffective tight reservoir, respectively. Among them, the classes I and II reservoirs were the sweet spot areas for increasing the reserves and production of tight oil. The method of combining various reservoir forming limits and pore structure types can effectively evaluate reservoir quality, and provide theoretical basis for increasing geological reserves and rolling expansion of oil fields.

Keywords: Tight oil reservoir; Pore structure type; Reservoir forming limit; Grading evaluation criteria; Ordos basin

1. Introduction

Recently, the innovation of tight oil accumulation theory and the successful application of hydraulic fracturing and sweet spot prediction techniques have sparked a global boom in tight oil development [1,2]. China has the world's third largest tight oil reserves after the United States and Russia, which have achieved large-scale commercial exploitation [3]. However, compared to tight oil in marine basins of the United States, the formation environment of continental tight oil in China was more complex, with diverse sedimentary types and systems, multi-stages adjustment and transformation of tectonic sedimentary evolution, and features of such as fine pore throats, poor fluid mobility, and low formation pressure [4–7]. Therefore, it is urgent to carry out pore structure and reservoir evaluation, which lay a foundation for the optimization of sweet spot areas and efficient development of tight oil.

* Corresponding author.

Presently, with the deepening of research on multi-scale pore structure and the mature application of various characterization techniques, the characterization of pore structure was developing towards more refined, quantified, high-precision, and full pore size directions [1,6,8–12]. Among these testing methods, high-pressure mercury injection (HPMI) testing can overcome the large capillary resistance and enter the nanoscale pore-throat space [9,13,14]. Moreover, this method has the characteristics of low-cost and high-efficiency, and was widely used in the classification research of pore structures [15,16]. In addition, the research on the reservoir forming limits of tight sandstone was mainly focused on determining of the pore-throat lower limit and petrophysical properties lower limit [11,17]. Among them, the theoretical pore-throat lower limit of current tight oil reservoirs was usually determined by the irreducible water film thickness method, and the petrophysical properties lower limit of oil and gas charged tight reservoirs was determined by various methods such as empirical statistics and oil testing productivity [18,19]. However, there were different types of the reservoir forming limits in tight sandstone reservoirs, and the petrophysical properties lower limit was not a constant value and will gradually decline with the improvement of the exploitation technology. Therefore, different methods should be used to determine the various reservoir forming limits when oil and gas charged the tight sandstone.

The reservoir evaluation was the prerequisite for predicting the sweet spot areas of tight oil, and its accuracy affects the selection of exploration targets and the assessment of oil and gas reserves [5,16,20,21]. At present, there are four categories of classification and evaluation methods for tight oil reservoirs, including petrophysical facies method, multi-parameter comprehensive evaluation method, pore structure classification method, and petrophysical properties lower limit method [22–24]. Among them, the petrophysical facies method can qualitatively evaluate the quality of reservoirs from the perspective of geological genesis, establish favorable petrophysical facies identification standards and evaluation systems, and clarify their planar distribution patterns [25,26]. However, this method was difficult to provide quantitative standards for reservoir classification and evaluation. The multi-parameter comprehensive evaluation method selects parameters representing the characteristics of tight oil reservoirs, such as lithology, petrophysical properties, and electrical properties, and adopts the evaluation methods such as the clustering analysis method and multivariate classification coefficient method to evaluate the reservoir differences in the target area [27]. However, these parameters and methods were difficult to establish unified standards for application in different target areas. The pore structure classification method selects various parameters obtained from each experiment to classify and evaluate the pore structure [28,29]. By analyzing the storage and permeability capacity under different pore structure types to evaluate the tight oil reservoirs. However, this method needs to carry out a large amount of analysis and testing, which is difficult to promote for blocks with low exploration degree or lack of relevant data. The petrophysical properties lower limits of different oil-bearing reservoirs were defined based on various static and dynamic methods such as empirical statistical method and oil-bearing occurrence method to complete the reservoir evaluation [30]. This method considers the effectiveness of storage and seepage capacity of reservoirs, but the classification results have certain statistical rules.

Therefore, in this study, 31 tight sandstone samples were selected and carried out testing on petrophysical properties and HPMI to classify and study the pore structure of reservoirs. In addition, the reservoir forming limits of tight sandstone were accurately determined through various methods. On this basis, various reservoir forming limits and pore structure types were combined to quantitatively evaluate tight oil reservoirs and establish the corresponding grading evaluation criteria, which provides a theoretical basis for increasing geological reserves and rolling expansion of the oil field.

2. Geological background

Ordos Basin is located in the middle of China (Fig. 1a) [31]. It is a Mesozoic sedimentary basin formed by overall uplift and subsidence, depression migration and long-term superposition evolution [32,33]. The basin spans five administrative regions and six first-order structural units [9,15]. After undergoing a long sedimentary evolution and tectonic movement in the basin, a nearly rectangular basin with a regional area of 25×10^4 km^2 has been formed (Fig. 1b) [15,34,35]. The structures of the basin were relatively simple, with a gentle westward dipping monoclinic structure and an inclination angle of less than 1 (Fig. 1c).

The Jiyuan area is located in the midwestern part of Ordos Basin, at the junction of Shaanxi, Gansu, and Ningxia provinces, with the regional exploration area covers 1,857 km^2 [36,37]. The overall performance of Chang 7 reservoir is characterized by a reverse sedimentary cycle of lake retreat and sand advance. Based on the characteristics of logging curves, the Chang 7 member can be divided into five sub-members, namely Chang 7_1^1, Chang 7_1^2, Chang 7_2^1, Chang 7_2^2, and Chang 7_3. Among them, the Chang 7_1^1 and Chang 7_1^2 sub-member are the main producing layers of Chang 7 tight oil and the target horizon of this study, with the average thickness of 6.84 and 7.45 m, respectively. The rock type of tight oil reservoir is lithic feldspar sandstone, with a high content of interstitites in the reservoir, averaging 15.77%, which mainly including illite in clay minerals and ferrocalcite in carbonate cements, with the average of 3.13% and 3.72%, respectively. The compositional maturity and structural maturity are both medium and low.

3. Experimental methods

In this paper, 31 tight sandstone core samples were selected and drilled parallel to the formation direction using a drilling rig to form cylindrical plugs with a diameter and length of about 2.5 cm. Then, the sample plugs were numbered individually and placed into alcohol and benzene for extraction experiments. After drying, the porosity, permeability, and HPMI experiments were conducted on the sample plugs to characterize the petrophysical properties and pore-throat size distribution (PSD) characteristics.

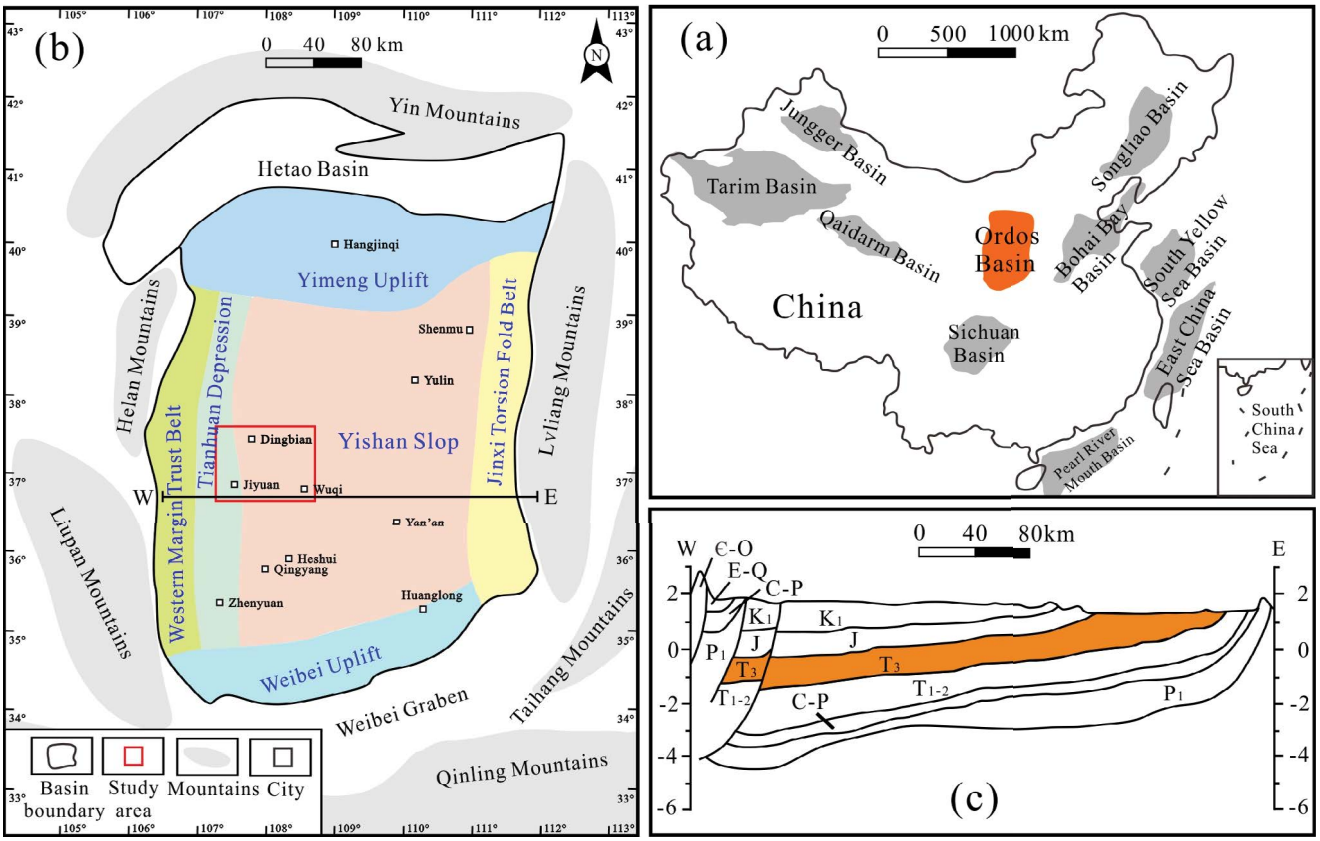

Fig. 1. (a) Location map of Ordos Basin, (b) tectonic division of Ordos Basin, and (c) structural section corresponding to horizontal line in Fig. 1b.

3.1. Porosity and permeability

The Smart-Por ultra-low porosity and Smart-Perm ultra-low permeability test systems developed by Tai-Rocky Tech System Company in Canada were used to complete the helium porosity and helium permeability test of rocks, respectively. The system can realize the automatic testing of tight sandstone samples under different confining pressures and pore pressures, with high test accuracy. The technical parameters of the system include a confining pressure of 0–75 MPa, a pore fluid pressure of 0.7–14 MPa, a porosity measurement range of 1%–20%, and a permeability measurement range of 0.0001–50 × 10^{-3} μm^2.

3.2. HPMI

HPMI experiments were performed using the Autopore 9250 II mercury porosimeter. During the experiments, the non-wetting phase of mercury was continuously pressurized under vacuum conditions, which allowed mercury to enter the reservoir space with a smaller pore-throat radius and recorded corresponding mercury saturation at stable pressures. Then the PSD characteristics of the sample were quantitatively detected based on the Washburn equation. The parameters of the HPMI experiments included the following: a pressure range of the mercury injection of 0–200.3 MPa and a measurement range of pore size of 0.0037–100 μm.

4. Results

4.1. Petrophysical properties

By analyzing the petrophysical properties data of 31 cores (Table 1), the porosity of Chang 7 tight oil reservoirs was scattered between 4.44% and 11.46%, averaging 8.02%, and the reservoir permeability was distributed between 0.033 and 1.001 × 10^{-3} μm^2, averaging 0.298 × 10^{-3} μm^2, which represents a typical tight sandstone reservoir. In addition, the petrophysical properties data of 3,387 cores collected from Chang 7_1^1 and Chang 7_1^2 reservoirs were analyzed. The porosity of Chang 7 tight oil reservoirs was mainly scattered between 6% and 12%, showing a normal distribution, of which the proportion of samples with porosity less than 10% accounts for 81.2% (Fig. 2a). The reservoir permeability was mainly distributed between 0.01 and 0.50 × 10^{-3} μm^2, in which 56.3% of the samples with permeability less than 0.1 × 10^{-3} μm^2 (Fig. 2b). Moreover, the distribution of porosity and permeability in Chang 7_1^1 reservoir was generally on the left, with poor petrophysical properties. The average values of porosity and permeability were 8.11% and 0.213 × 10^{-3} μm^2, respectively, and the correlation between the two was relatively weak, with correlation coefficient (R^2) being 0.6459 (Fig. 2c). The average values of porosity and permeability in Chang 7_1^2 reservoir were 8.90% and 0.269 × 10^{-3} μm^2, respectively, and the correlation between them was better, with a R^2 of 0.7544 (Fig. 2d), indicating that the overall quality of

Table 1
Four types of pore structure parameters obtained from HPMI experiment

Pore structure types	Sample ID	Porosity (%)	Permeability (10^{-3} μm^2)	P_d (MPa)	R_{max} (μm)	R_a (μm)	S_{max} (%)	W_e (%)	S_p	α
Type I	L197	9.96	0.545	0.72	1.02	0.25	92.43	34.41	0.25	1.93
	L50	9.89	0.893	0.46	1.60	0.43	90.26	28.11	0.27	2.19
	L54	11.46	1.001	0.27	2.68	0.54	88.15	34.19	0.20	2.74
	Y153	8.85	0.442	0.72	1.02	0.26	88.92	35.50	0.25	2.33
	H343	10.02	0.768	0.46	1.61	0.33	87.68	33.74	0.21	2.45
	G203	10.49	0.867	0.45	1.62	0.43	92.56	34.91	0.27	2.19
	H513-1	11.15	0.552	0.67	1.09	0.24	92.91	36.64	0.16	2.40
	Average	10.26	0.724	0.54	1.52	0.34	90.42	33.93	2.32	0.23
Type II	F89	8.54	0.192	1.17	0.63	0.12	91.91	39.19	0.20	1.97
	G273	8.40	0.320	0.72	1.02	0.24	90.53	33.21	0.23	2.12
	G275	9.54	0.283	1.17	0.63	0.12	91.91	41.96	0.19	2.00
	H359	8.30	0.237	0.72	1.02	0.10	72.28	40.52	0.10	3.66
	L36	9.80	0.454	0.74	1.00	0.18	92.56	41.25	0.18	2.03
	H370	10.47	0.343	1.14	0.64	0.12	87.30	34.54	0.15	2.39
	H395	7.74	0.236	1.17	0.63	0.12	83.13	24.22	0.15	2.78
	C223	8.99	0.566	0.72	1.02	0.15	96.82	45.78	0.15	1.77
	Average	8.97	0.329	0.94	0.82	0.15	88.30	37.58	2.34	0.17
Type III	G282	7.90	0.140	1.81	0.41	0.08	86.17	31.39	0.20	2.17
	G345	6.70	0.100	2.91	0.25	0.07	90.14	37.83	0.28	1.85
	G91	5.92	0.060	2.91	0.25	0.05	87.19	38.39	0.19	2.07
	G71	7.15	0.121	1.81	0.41	0.09	84.51	26.70	0.21	2.46
	H136	6.50	0.101	1.16	0.63	0.08	77.87	33.04	0.17	2.85
	H152	5.85	0.091	2.91	0.25	0.04	88.81	34.86	0.16	1.79
	H415	7.55	0.096	2.08	0.35	0.10	90.58	28.29	0.29	2.09
	H513-2	7.87	0.183	2.75	0.27	0.09	89.89	26.73	0.32	2.09
	L152	8.30	0.148	1.37	0.54	0.10	87.37	32.10	0.31	2.29
	L184	6.43	0.057	2.05	0.36	0.06	90.78	28.92	0.30	2.08
	L187	7.60	0.143	1.17	0.63	0.10	86.82	24.89	0.22	2.38
	L22	7.47	0.115	1.81	0.41	0.06	91.03	40.70	0.15	1.76
	Average	7.10	0.113	2.06	0.40	0.09	87.60	31.99	2.16	0.23
Type IV	D308	5.60	0.052	7.39	0.10	0.02	45.29	13.56	0.19	4.92
	H195	4.58	0.054	2.91	0.25	0.03	70.40	16.91	0.12	3.92
	H212	5.02	0.042	2.91	0.16	0.03	62.00	19.19	0.16	4.88
	H211	4.44	0.033	11.78	0.06	0.02	40.92	7.43	0.19	6.00
	Average	4.91	0.045	6.25	0.14	0.02	54.65	14.27	4.93	0.16

the Chang 7_1^2 reservoir was better than those of the Chang 7_1^1 reservoir. This was because that the depositional hydrodynamics and sand body development scale of Chang 7_1^1 reservoir was weaker than that of Chang 7_1^2 reservoir.

4.2. Classification and characteristics of pore structure

The HPMI results showed that the pore structure of Chang 7 tight oil reservoir was poor, with a higher displacement pressure (P_d) and a smaller pore-throat radius (R_a) (Fig. 3). The distribution of P_d was between 0.27 and 11.78 MPa, averaging 1.97 MPa, and the R_a was distributed between 3.6 nm and 4.0 μm, averaging 0.15 μm (Table 1). By analyzing the pore structure parameters of each sample, it was found that the pore structure has obvious boundaries at the P_d of 0.72, 1.17, 2.91 MPa, and the R_a of 0.24, 0.12, 0.03 μm, while other pore structure parameters have significant differences among various sandstone samples, indicating that tight oil reservoirs have complex configuration relationships and heterogeneous of pore throats. Therefore, according to the morphological characteristics of capillary pressure curves, PSD characteristics, and pore structure parameters obtained by HPMI, the pore structure was divided into four types: I, II, III, and IV.

Among these types, the capillary pressure curve distribution uplifted gradually and the P_d increased successively, with average values of 0.54, 0.94, 2.06, and 6.25 MPa (Fig. 4). The corresponding PSD curves showed a unimodal

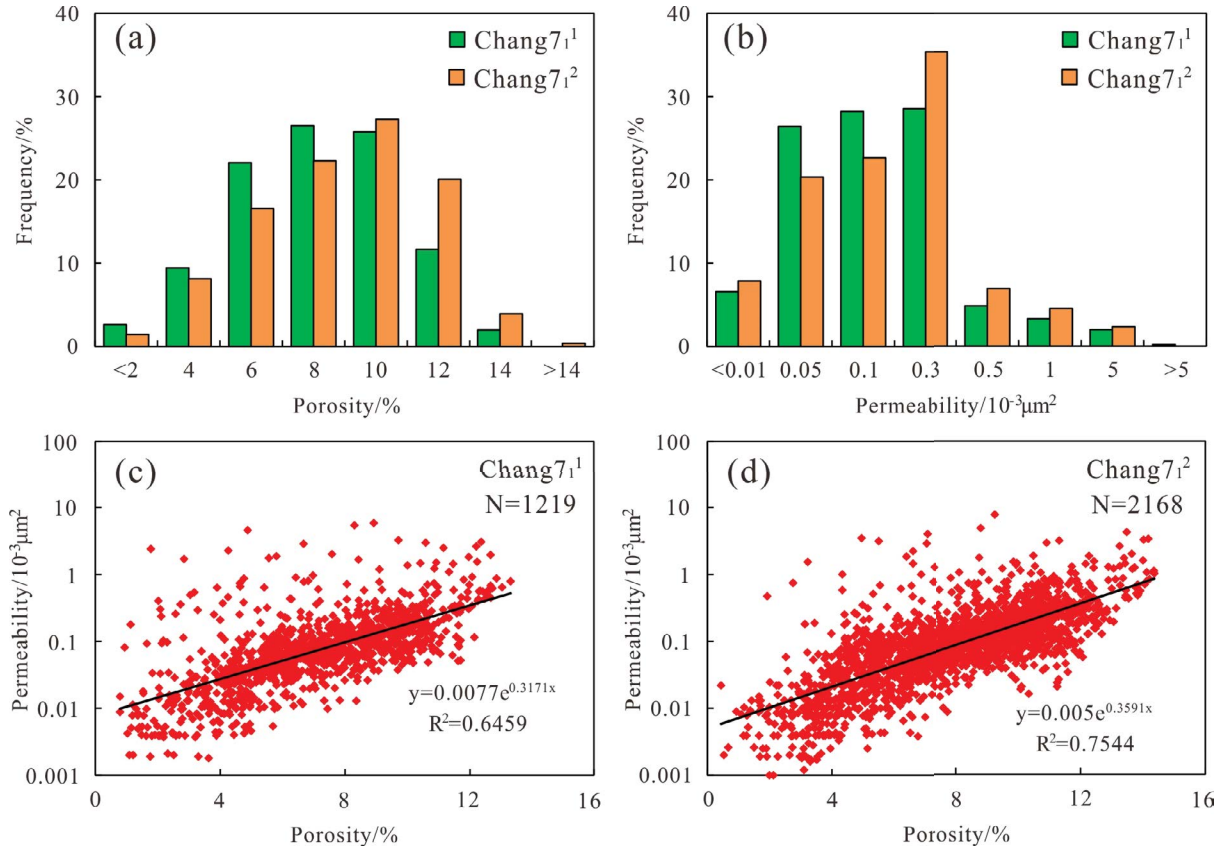

Fig. 2. Histogram of petrophysical property distribution of Chang 7_1^1 and Chang 7_1^2 reservoirs (a,b) and intersection diagram of porosity and permeability (c,d).

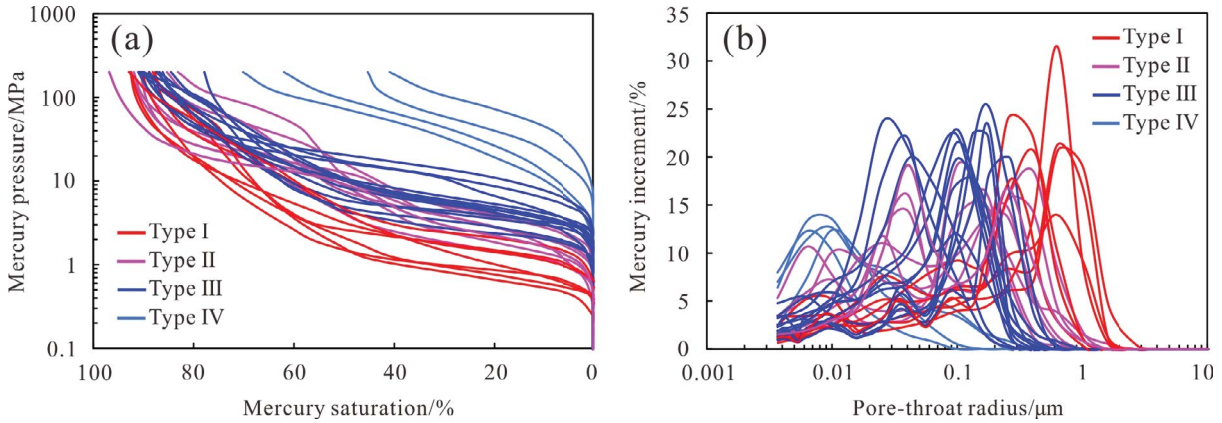

Fig. 3. Capillary pressure curve characteristics (a) and PSD characteristics (b) obtained from HPMI.

distribution and gradually shifted to the left, and the R_a gradually decreased, with average value of 0.34, 0.15, 0.09, and 0.02 μm. The pore-throat combination type transitions from residual intergranular pores and feldspar dissolution pores to intercrystalline pores, and the rock gradually becomes dense. Moreover, the maximum mercury injection saturation (S_{max}) and mercury withdraw efficiency (W_e) of type I pore structure have average values of 90.42% and 33.93%, respectively, and the sorting coefficient (S_p) and homogeneity coefficient (α) of the PSD have average values of 2.32 and 0.23, respectively. This indicates that this type of sample develops larger pore throats and the PSD was relatively concentrated and uniformly distributed, thereby corresponding to a higher reservoir space and seepage capacity. The PSD of type II pore structure showed a wide and slow single-peak characteristic, with a high S_p and a low α (average values were 2.34 and 0.17, respectively). Meanwhile, the type II pore structure had larger S_{max} and the highest W_e (average values were 88.30% and 37.58%, respectively), indicating that this type of sample had a better configuration relationship and connectivity

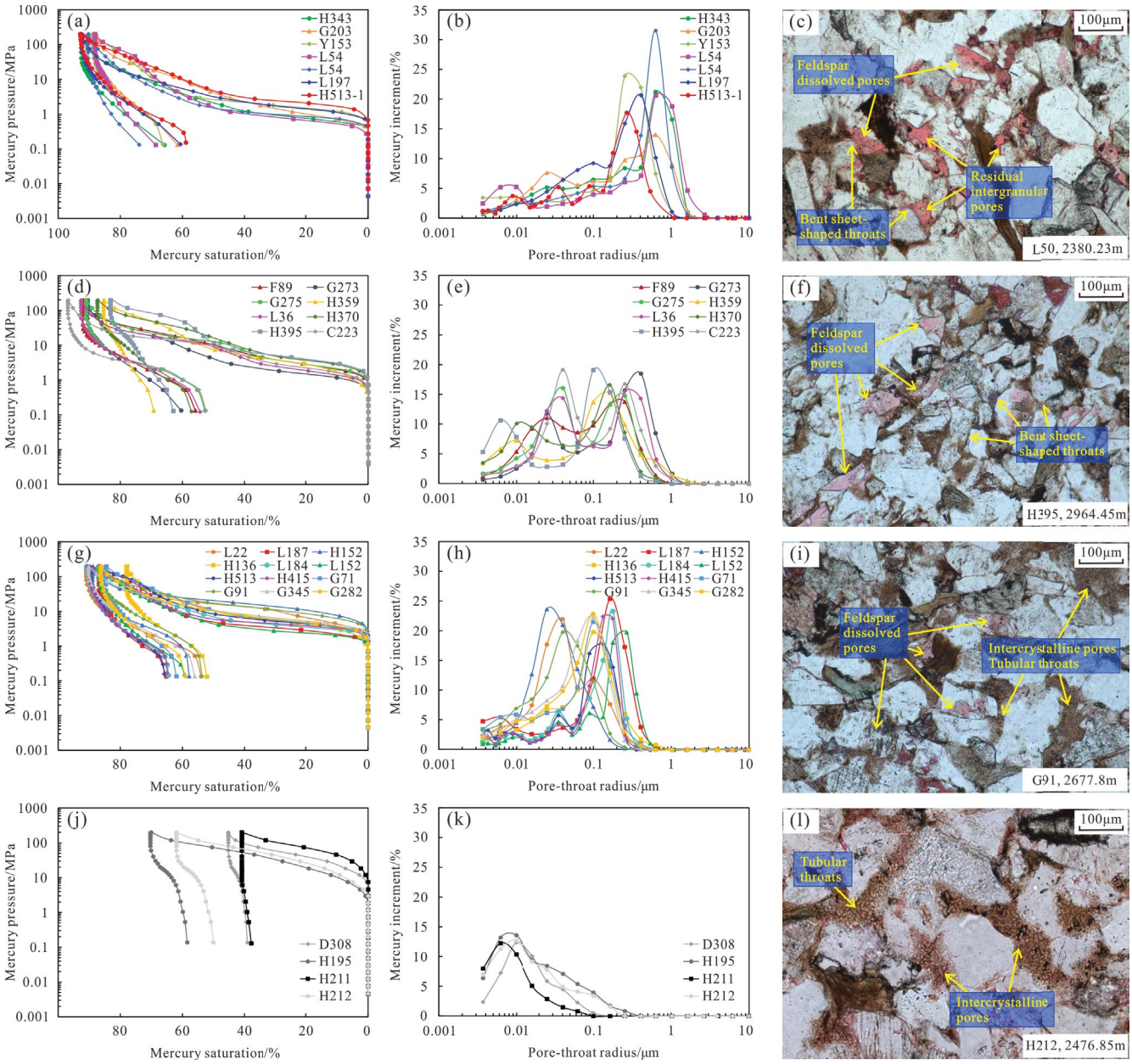

Fig. 4. Differences in pore structure of tight oil reservoirs.

of the pore throats. Type III pore structure had a small pore-throat radius, a concentrated distribution, the lowest S_p, and the highest α (average values were 2.16 and 0.23, respectively), corresponding to a lower S_{max} and W_e (average values were 87.60% and 31.99%, respectively). The type IV pore structure had the highest S_p and the lowest α (average values were 4.93 and 0.16, respectively). This type of sample developed tinier pore throats and showed the lowest effective volume and configuration relationship of pore-throat space (average values of S_{max} and W_e were 54.65% and 14.27%, respectively).

4.3. Classification of reservoir forming limits

There are different lower limits of pore-throat radius or petrophysical properties during the oil and gas enter the reservoirs, which can be called the reservoir forming limits of tight sandstone [11,19]. The specific reservoir forming limits include the theoretical lower limit, lower limit of oil accumulation, and effective seepage lower limit (Fig. 5). Among them, the theoretical lower limit refers to the lower limits of pore-throat radius or petrophysical properties corresponding to the oil and gas can pass through the source-reservoir interface, when the accumulation dynamic fails to overcome the capillary resistance of the pore throats, the oil and gas cannot be charged into the reservoir, which was defined as non-reservoir [38]. The lower limit of oil accumulation represents the petrophysical properties of the corresponding reservoir where oil and gas can be filled into tight rocks under the action of accumulation dynamics [39]. When the petrophysical properties of the reservoir

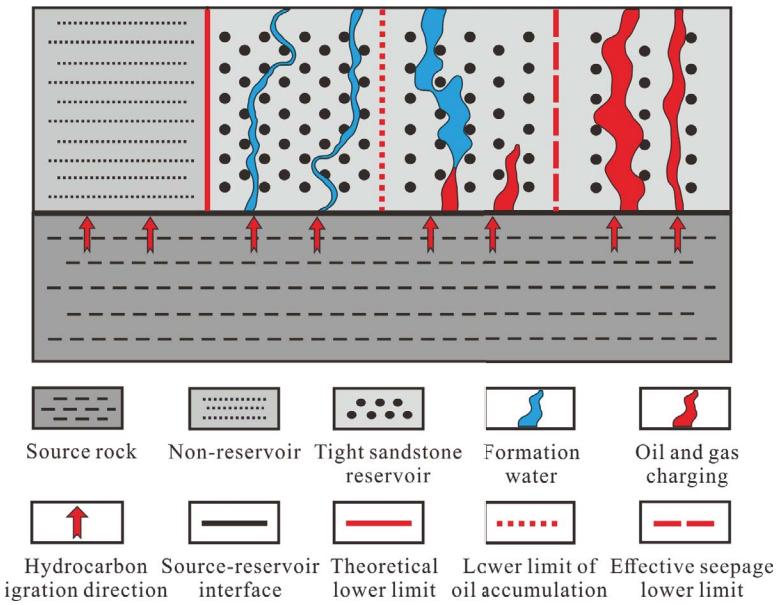

Fig. 5. Distribution diagram of reservoir forming limits of tight sandstone.

were less than this critical value, there was no oil and gas display, and the reservoir was considered as the ineffective tight reservoir, which was occupied by the original formation water [17,40]. Although the oil and gas can enter the sandstone to form the oil-bearing tight reservoir, some tight oils were difficult to flow effectively. Therefore, the effective seepage lower limit reflects the petrophysical properties corresponding to the flow of tight oil in pores, which was also known as the industrial lower limit, and this limit decreases with the improvement of the exploitation technology [14,41]. The above analysis shows that tight oil reservoirs have different reservoir forming limits, corresponding to reservoirs with different petrophysical properties and pore structures, which have absolute control over the oil accumulation.

4.3.1. Theoretical lower limit

Before hydrocarbons enter the reservoir space, the original formation pores contain water. Due to factors such as electrostatic field, wettability, and clay adsorption, the mineral surface usually adsorbs a certain thickness of water film [42]. When the sum of the irreducible water film and oil molecules radius were equal to the pore-throat radius, which was the theoretical lower limit of pore-throat corresponding to oil and gas charging [43]. Since the oil-water interfacial tension decreases with the increase of formation pressure and temperature, it is necessary to establish the relationship diagram between the pore-throat radius and the irreducible water film thickness under different formation pressures (Fig. 6a). The critical thickness of water film under different formation pressures were fitted to obtain the irreducible water film thickness under the current formation pressure of study area (Fig. 6b). The current formation pressure is 24 MPa, and the corresponding critical thickness is 14 nm. Due to the oil molecular radius is 1.3 nm on average, the theoretical lower limit of pore-throat of study area can be determined to be 15.3 nm. Therefore, according to the correlation between permeability and R_a and porosity (Fig. 6c and d), the corresponding lower limit of porosity and permeability was determined to be 3.5% and 0.02×10^{-3} μm^2, respectively.

4.3.2. Lower limit of oil accumulation

When oil and gas overcame the resistance of the small throats at the source-reservoir interface and entered the interior of the reservoir, due to the complex pore structure and strong reservoir heterogeneity, resulting in no oil and gas display inside some reservoirs [44,45]. Therefore, the lower limit of oil accumulation can be determined by the oil-bearing occurrence of tight sandstone. Predecessors classified oil-bearing occurrence into various types based on the degree of oil content in rock cores [46,47]. Among them, the oil-bearing reservoirs with oil saturated, oil rich, oil immersion, or oil spot have a higher oil-producing capacity and can be developed as industrial oil reservoirs [48]. Reservoirs with oil spot or oil stain have a lower oil-producing capacity and were considered as low-producing oil layers [49]. However, reservoirs with fluorescence were basically unable to store and produce oil and gas, making them as the dry reservoirs. Therefore, the petrophysical property boundary between oil free and other oil-bearing grades can be used as the lower limit of oil accumulation. Based on 227 core petrophysical property data points and debris data from 30 exploration wells, the intersection diagram of porosity and permeability of cores with different oil-bearing levels was established (Fig. 7). The analysis results indicate that the better the petrophysical properties of reservoirs, the higher the oil-bearing grade in the sandstone. The porosity and permeability limits of oil-bearing sandstone samples were 5.5% and 0.05×10^{-3} μm^2, respectively.

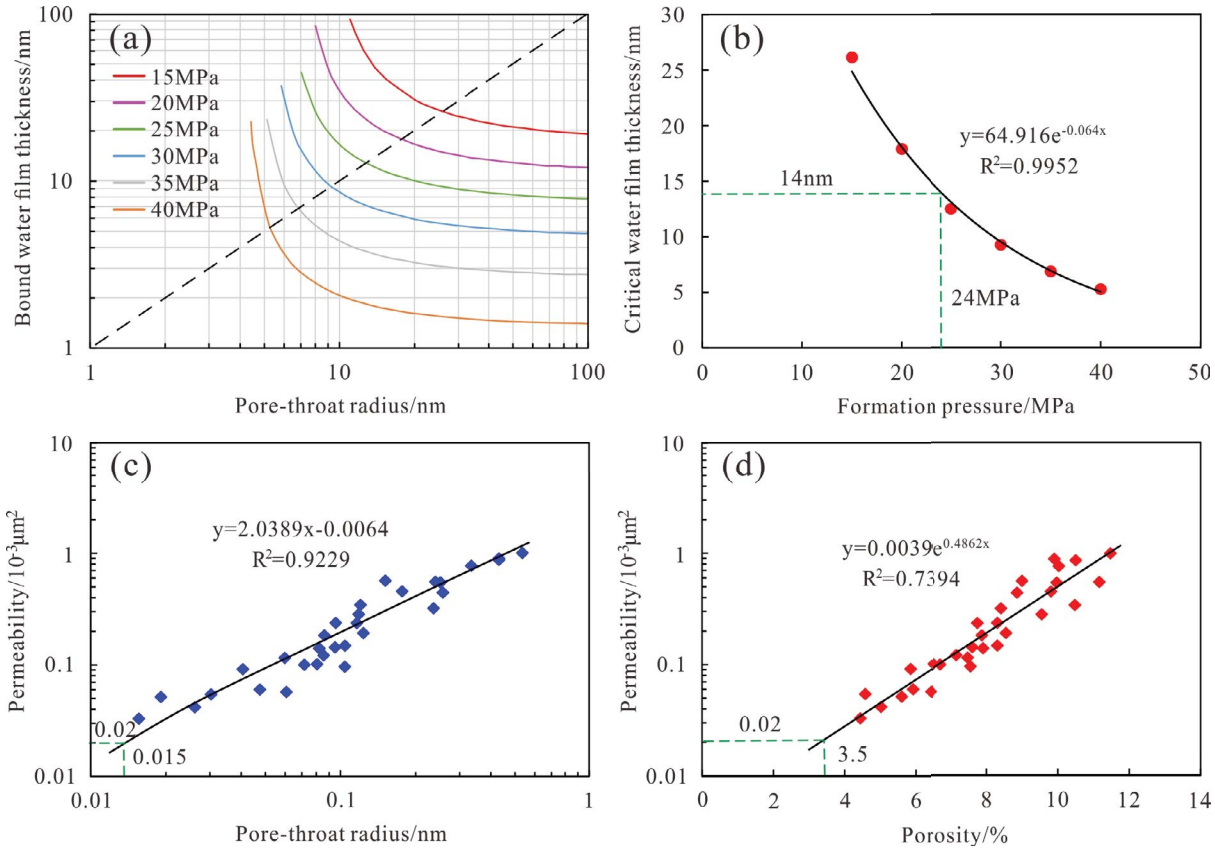

Fig. 6. Theoretical lower limit was obtained by irreducible water film thickness method.

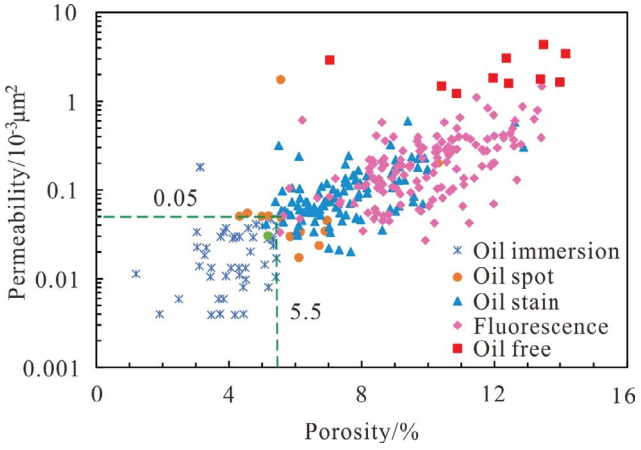

Fig. 7. Petrophysical properties correlation of cores with different oil-bearing occurrences.

4.3.3. *Effective seepage lower limit*

The effective seepage lower limit was the petrophysical property lower limit of the effective tight oil production layers [50,51]. This lower limit was the key to the screening of tight oil favorable areas and the formulation of later development measures [52]. The results of oil testing can usually comprehensively evaluate whether tight oil reservoirs have the development potential. In this method, the daily oil production and daily water production of the oil testing section were used as the basis for dividing the production layer (oil layer and water layer) and dry layer [43,53]. The intersection diagram of porosity and permeability was established based on the average petrophysical properties of different oil testing sections, and the petrophysical property boundary between the production layer and dry layer was used as the effective seepage lower limit. According to the oil testing results and petrophysical properties data of 99 wells, the intersection diagram of porosity and permeability was drawn for the oil testing section (Fig. 8). Analysis shows that there is a clear boundary in the distribution of petrophysical properties between the producing and dry layers of tight oil reservoirs, the corresponding lower limit of porosity and permeability were 8.0% and 0.20 × 10^{-3} μm^2, respectively. At the same time, it was found that the porosity distribution range of oil layer and water layer in tight oil production layer was similar, but the permeability of oil layer was higher than that of water layer, indicating that the oil-bearing property was controlled by the permeability.

5. Discussion

5.1. *Relationship between the reservoir forming limits and the classification boundaries of pore structure*

The study results in Section 4.2 indicates that the R_a of 0.24, 0.12 and 0.03 μm can be used as the boundary values of each pore structure type, which can be divided into four

types (I, II, III, and IV). simultaneously, a good correlation between permeability and R_a and porosity (Fig. 9), and the sample points represented by various pore structures have obvious differentiation. Therefore, the petrophysical property limits of various pore structures were determined based on the boundary value of the R_a, where the permeability limits corresponding to each pore structure were 0.50×10^{-3} μm², 0.20×10^{-3} μm², and 0.05×10^{-3} μm², and the corresponding porosity limits were 10.0%, 8.0%, and 5.5%, respectively.

In Section 4.3, there are three types of the reservoir forming limits in the Chang 7 tight sandstone reservoirs, namely the theoretical lower limit, lower limit of oil accumulation, and effective seepage lower limit, with the corresponding porosity limits of 3.5%, 5.5%, and 8.0%, respectively, and the corresponding permeability limits of 0.02×10^{-3} μm², 0.05×10^{-3} μm², and 0.20×10^{-3} μm², respectively. By comparing various reservoir forming limits with the pore structure classification boundaries, it was found that there is a good correlation between the two kinds of boundaries. Among them, the petrophysical property boundary between types II and III pore structures was the same as the effective seepage lower limit, the corresponding porosity and permeability were 8.0% and 0.2×10^{-3} μm², respectively, and the boundary between types III and IV pore structures was consistent with the lower limit of oil accumulation, the corresponding porosity and permeability were 5.5% and $0.0.05 \times 10^{-3}$ μm², respectively. This indicates that tight oil reservoirs of different oil grades can be formed when oil and gas enter reservoirs with different pore structures types and corresponding petrophysical properties, and also indicates that pore structure types can be used as the basis for classification of tight oil reservoirs.

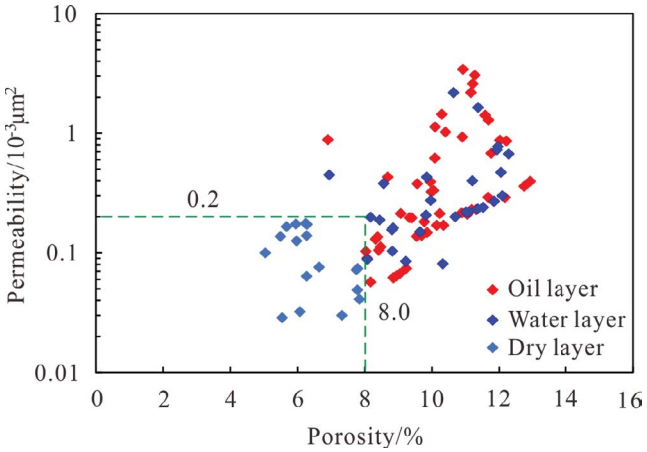

Fig. 8. Intersection diagram of porosity and permeability of the oil testing section.

5.2. Establishment of reservoir grading evaluation criteria and reservoir classification

The pore structure was the main factor affecting the petrophysical properties, fluid mobility and quality of tight oil reservoir [13,19]. Therefore, tight oil reservoirs can be graded and evaluated based on the type of pore structure. In addition, the porosity and permeability were usually used as the main parameters to evaluate the quality of tight oil reservoirs, and classified by clustering analysis and other methods [14,40]. However, the obtained petrophysical propertied boundary was only a statistical result and has no practical geological significance. Therefore, in this paper, the grading limits of tight oil reservoirs were determined by combining pore structure types and reservoir forming limits to clarify the geological significance represented by each grading limits.

In Section 4.3, various reservoir forming limits were determined through different methods, the Chang 7 tight oil reservoirs were divided into three types of reservoirs with different oil-bearing grades, namely effective tight reservoir, oil-bearing tight reservoir, and ineffective tight reservoir, which were distinguished from non-reservoir. Due to the reservoir forming limits were in good agreement with the classification boundaries of pore structure. Therefore, based on the combination of pore structure types and reservoir forming limits, the grading evaluation criteria for tight oil reservoirs were established (Table 2).

In order to better understand the geological significance of various tight oil reservoirs, combined with the fluid mobility corresponding to types I and II pore structures, the effective tight reservoirs were subdivided into easily movable

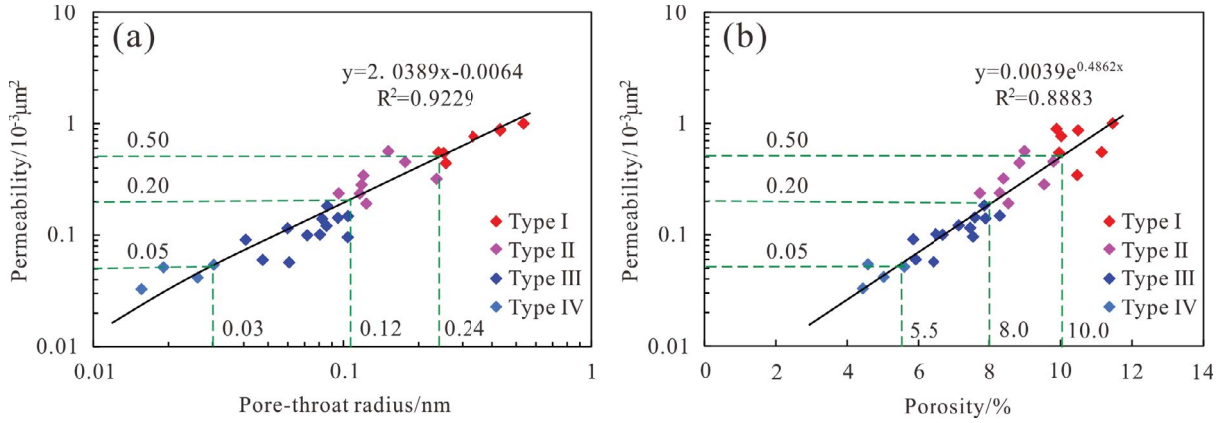

Fig. 9. Relationship between permeability and R_a (a) and porosity (b).

Table 2
Grading limits of tight oil reservoirs were determined by combining pore structure types and reservoir forming limits

Reservoir classification	Pore structure types	Geological significance	R_a (μm)	Permeability (10^{-3} μm^2)	Porosity (%)	Reservoir forming limits
Class I	Type I	Easily movable tight reservoir	>0.24	>0.50	>10.0	Effective seepage lower limit
Class II	Type II	Movable tight reservoir	0.12–0.24	0.20–0.50	8.0–10.0	
Class III	Type III	Oil-bearing tight reservoir	0.03–0.12	0.05–0.20	5.5–8.0	Lower limit of oil accumulation
Class IV	Type IV	Ineffective tight reservoir	0.015–0.03	0.02–0.05	3.5–5.5	
Non-reservoir	–	–	<0.015	<0.02	<3.5	Theoretical lower limit

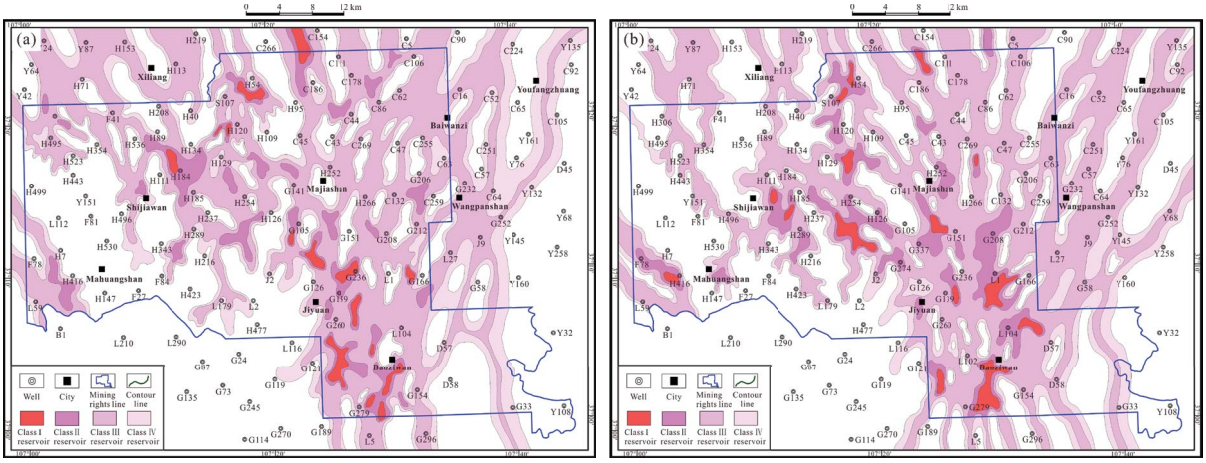

Fig. 10. Distribution plan of tight oil reservoir grading evaluation for Chang 7_1^1 (a) and Chang 7_1^2 (b).

tight reservoirs and movable tight reservoirs. According to the grading evaluation criteria, the tight oil reservoirs can be correspondingly divided into four classes (I, II, III, and IV), which were consistent with various pore structures, representing easily movable tight reservoirs, movable tight reservoirs, oil-bearing tight reservoirs, and ineffective tight reservoirs, respectively. Among them, class IV tight oil reservoirs have the small pore-throat radius, and correspond to porosity and permeability ranging from 3.5% to 5.5% and 0.02 to 0.05 × 10^{-3} μm^2, respectively, which represents ineffective tight reservoirs, and the boundary between it and non-reservoirs corresponds to the theoretical lower limit. Class III tight oil reservoirs were oil-bearing tight reservoirs, with corresponding porosity and permeability ranging from 5.5% to 8.0% and 0.05 to 0.20 × 10^{-3} μm^2, respectively. It was difficult for the fluids to flow effectively in this reservoir, and the boundary between this class and class IV tight oil reservoir corresponds to the lower limit of oil accumulation. Class II tight oil reservoirs were the movable tight reservoir, with better pore-throat configuration relationship, the corresponding porosity and permeability were between 8%–10% and 0.20–0.50 × 10^{-3} μm^2, respectively, and the boundary between it and the class III tight oil reservoir corresponds to the effective seepage lower limit. The class I tight oil reservoirs were the high-quality reservoir with the best reservoir performance and seepage capacity, and the corresponding porosity and permeability were greater than 10% and 0.50 × 10^{-3} μm^2, respectively, which represents the easily movable tight reservoir.

5.3. Application of reservoir grading evaluation criteria

The reservoir evaluation criteria were established based on the analysis and testing results of limited samples, but they were difficult to apply effectively in practice [36]. Therefore, it is necessary to combine rich logging data to better evaluate and predict the quality and distribution patterns of tight oil reservoirs. According to the corrected porosity and permeability logging curves, combined with the reservoir grading evaluation criteria, this paper can draw the distribution plan of grading evaluation for Chang 7_1^1 and Chang 7_1^2 tight oil reservoir (Fig. 10).

Fig. 10 shows that the Chang 7_1^1 and Chang 7_1^2 tight oil reservoirs were mainly distributed as class III reservoirs. The distribution characteristics of classes III and IV tight oil reservoirs were consistent with the distribution patterns of sand bodies and petrophysical properties, with a strip-shaped distribution along the provenance direction, mainly

distributed in underwater distributary channels and subaqueous natural levee. Among them, class IV tight oil reservoirs were distributed at the edge of distributary bays, corresponding to the worst reservoir petrophysical properties and pore structures, which were the areas that should be avoided for tight oil development. The classes I and II tight oil reservoirs were mainly scattered in the Jiyuan – Baoziwan area at the intersection of the southern dual provenance, with high oil and gas enrichment degree and fluid mobility, they were the favorable targets area for increasing the reserves and production of tight oil.

6. Conclusion

- The average porosity and permeability of Chang 7 tight oil reservoir were 8.02% and 0.298 × 10^{-3} μm², respectively. According to the capillary pressure curve morphology, P_d (0.72, 1.17, and 2.91 MPa), and R_a (0.24, 0.12, and 0.03 μm), the pore structure can be divided into four types (I, II, III, and IV), where the R_a and the oil-bearing properties of the reservoir gradually decreases.
- The Chang 7 tight oil reservoir has the three reservoir forming limits, namely the theoretical lower limit, lower limit of oil accumulation, and effective seepage lower limit, the corresponding lower limits of porosity were 3.5%, 5.5%, and 8%, respectively, and the corresponding lower limits of permeability were 0.02 × 10^{-3} μm², 0.05 × 10^{-3} μm², and 0.20 × 10^{-3} μm², respectively.
- There was a good correspondence between the various reservoir forming limits and the classification boundaries of pore structure, the Chang 7 tight oil reservoirs can be divided into four classes by combining these two types of boundaries, and the corresponding grading evaluation criteria can effectively predict the favorable sweet spot areas in the Jiyuan area. Among them, class I reservoir reflects easily movable tight reservoir, corresponding to the best reservoir quality and development potential. Class II reservoir represents movable tight reservoir, and the boundary between it and class III reservoir corresponds to the effective seepage lower limit. Class III reservoir represents the oil-bearing tight reservoir, which was the main reservoir type in Jiyuan area. Class IV reservoir was shown as an ineffective tight reservoir, which contributes little to the production of the tight oil reservoir.

Acknowledgments

Thanks to China Shaanxi Yanchang Petroleum (Group) Company for providing the samples and related materials.

References

[1] Q.P. Zhang, Y.C. Liu, B.T. Wang, J.F. Ruan, N. Yan, H. Chen, Q. Wang, G.W. Jia, R.N. Wang, H. Liu, C.W. Xue, F.L. Liu, H. Yang, Y.S. Zhu, Effects of pore-throat structures on the fluid mobility in Chang 7 tight sandstone reservoirs of longdong area, Ordos Basin, Mar. Pet. Geol., 135 (2022) 105407, doi: 10.1016/j.marpetgeo.2021.105407.

[2] X.Y. Zhong, Y.S. Zhu, L.P. Liu, H.M. Yang, Y.F. Li, Y.H. Xie, L.Y. Liu, The characteristics and influencing factors of permeability stress sensitivity of tight sandstone reservoirs, J. Pet. Sci. Eng., 191 (2020) 107221, doi: 10.1016/j.petrol.2020.107221.

[3] L.D. Sun, C.N. Zou, A.L. Jia, Y.S. Wei, R.K. Zhu, S.T. Wu, Z. Guo, Development characteristics and orientation of tight oil and gas in China, Pet. Explor. Dev., 46 (2019) 1073–1087.

[4] X.S. Lu, M.J. Zhao, K.Y. Liu, Q.G. Zhuo, J.J. Fan, Z.C. Yu, Y.J. Gong, Formation condition of deep gas reservoirs in tight sandstones in Kuqa Foreland Basin, Pet. Res., 3 (2018) 346–358.

[5] X. Fang, Z. Yang, W.P. Yan, X.G. Guo, Y.X. Wu, J.T. Liu, Classification evaluation criteria and exploration potential of tight oil resources in key basins of China, J. Nat. Gas Geosci., 4 (2019) 309–319.

[6] P. Li, C.Z. Jia, Z.J. Jin, Q.Y. Liu, H. Bi, M. Zheng, S.T. Wu, Z.K. Huang, Pore size distribution of a tight sandstone reservoir and its effect on micro pore-throat structure: a case study of the Chang 7 member of the Xin'anbian Block, Ordos Basin, China, Acta Geol. Sin., 94 (2020) 219–232.

[7] X.X. Wang, J.G. Hou, Y.M. Liu, P.Q. Zhao, K. Ma, D.M. Wang, X.X. Ren, L. Yan, Overall PSD and fractal characteristics of tight oil reservoirs: a case study of Lucaogou Formation in Junggar Basin, China, Fractals, 27 (2019) 1940005, doi: 10.1142/S0218348X1940005X.

[8] D.T. Li, Z.L. He, S.Z. Sun, C. Wang, W.Q. Chen, Z.W. Xing, Development and analysis of novel six-lobe helical rotors for hydrogen fuel cell vehicle roots blowers, Int. J. Hydrogen Energy, 46 (2021) 30479–30493.

[9] X.L. Zhao, Z.M. Yang, S.B. Zhou, Y.T. Luo, X.W. Liu, Y.P. Zhang, W. Lin, Q.H. Xiao, Z.K. Niu, Research on characterization and heterogeneity of microscopic pore throat structures in tight oil reservoirs, ACS Omega, 6 (2021) 24672–24682.

[10] S. Yin, L. Dong, X. Yang, R. Wang, Experimental investigation of the petrophysical properties, minerals, elements and pore structures in tight sandstones, J. Nat. Gas Sci. Eng., 76 (2020) 103189, doi: 10.1016/j.jngse.2020.103189.

[11] W.M. Wang, Y.N. Liu, C.S. Miao, Y.H. Liu, X.Y. Qu, Y.C. Zhang, W.H. La, Q.X. Lv, Ranking and evaluation of tight sandstone reservoirs and the determination of the lower limit of reservoir physical properties: a case study of Longfengshan Area in the Southern Songliao Basin, China, Geofluids, 2022 (2022) 9889714, doi: 10.1155/2022/9889714.

[12] Y. Xin, G.W. Wang, B.C. Liu, Y. Ai, D.Y. Cai, S.W. Yang, H.K. Liu, Y.Q. Xie, K.J. Chen, Pore structure evaluation in ultra-deep tight sandstones using NMR measurements and fractal analysis, J. Pet. Sci. Eng., 211 (2022) 110180, doi: 10.1016/j.petrol.2022.110180.

[13] W.R. Wang, D. Yue, K.A. Eriksson, X.F. Qu, W. Li, M. Lv, J.Q. Zhang, X.T. Zhang, Quantification and prediction of pore structures in tight oil reservoirs based on multifractal dimensions from integrated pressure- and rate-controlled porosimetry for the Upper Triassic Yanchang Formation, Ordos Basin, China, Energy Fuels, 34 (2020) 4366–4383.

[14] S.Q. Ouyang, X.X. Lü, Y.Y. Zhang, L. Chen, Y.Q. Qu, W. Sun, Impacts of the pore–throat structure on fluid mobility in tight sandstone: insight from an improved method based on rate-controlled porosimetry and nuclear magnetic resonance, Energy Fuels, 37 (2022) 273–290.

[15] Z.J. Xu, L.F. Liu, T.G. Wang, K.J. Wu, W.C. Dou, X.P. Song, C.Y. Feng, X.Z. Li, H.T. Ji, Y.S. Yang, X.X. Liu, Characteristics and controlling factors of lacustrine tight oil reservoirs of the Triassic Yanchang Formation Chang 7 in the Ordos Basin, China, Mar. Pet. Geol., 82 (2017) 265–296.

[16] S.F. Lu, J.Q. Li, D.S. Xiao, H.T. Xue, P.F. Zhang, J.J. Li, F.W. Chen, W.B. Huang, M. Wang, W.H. Li, Z.C. Li, Research progress of microscopic pore–throat classification and grading evaluation of shale reservoirs: a minireview, Energy Fuels, 36 (2022) 4677–4690.

[17] L. Wang, Y.F. Zhang, R.L. Luo, R. Zou, H. Deng, R. Zou, L. Huang, Y.S. Liu, Lower limits of petrophysical parameters for effective reservoirs in ultradeep carbonate gas reservoirs: a case study from the Deng IV Member, Gaoshiti-Moxi Area, Sichuan Basin, SW China, J. Hydrol., 621 (2023) 129657, doi: 10.1016/j.jhydrol.2023.129657.

[18] L.X. Cai, X.W. Guo, X.H. Zhang, Z.G. Zeng, G.L. Xiao, Y.M. Pang, S.P. Wang, Pore-throat structures of the Permian Longtan Formation tight sandstones in the South Yellow Sea Basin, China: a case study from borehole CSDP-2, J. Pet. Sci. Eng., 186 (2020) 106733, doi: 10.1016/j.petrol.2019.106733.
[19] F.W. Wang, D.X. Chen, D.S. Yao, M. Cheng, Q.C. Wang, Z.Y. Tian, W.L. Du, C. Wang, S.Y. Chang, M.Y. Jiang, Disparities in tight sandstone reservoirs in different source-reservoir assemblages and their effect on tight oil accumulation: Triassic Chang 7 member in the Qingcheng area, Ordos Basin, J. Pet. Sci. Eng., 217 (2022) 110914, doi: 10.1016/j.petrol.2022.110914.
[20] H.T. Gao, X.P. Zhou, Z.G. Wen, W. Guo, W.C. Tian, S.X. Li, Y.P. Fan, Y.S. Luo, Classification and evaluation of shale oil reservoirs of the Chang 7_{1-2} sub-member in the Longdong Area, Energies, 15 (2022) 5364, doi: 10.3390/en15155364.
[21] N.W. Zhou, S.F. Lu, M. Wang, W.B. Huang, D.S. Xiao, C.X. Jiao, J.M. Wang, W.C. Tian, L. Zhou, F.W. Chen, W. Liu, Z.X. Wang, Limits and grading evaluation criteria of tight oil reservoirs in typical continental basins of China, Pet. Explor. Dev., 48 (2021) 1089–1100.
[22] Q. Dai, Q. Luo, C. Zhang, C. Lu, Y. Zhang, S. Lu, Y. Zhao, Pore structure characteristics of tight-oil sandstone reservoir based on a new parameter measured by NMR experiment: a case study of seventh Member in Yanchang Formation, Ordos Basin, Acta Pet. Sin., 37 (2016) 887–897.
[23] B.Y. Ma, Q.H. Hu, S.Y. Yang, T. Zhang, H.G. Qiao, M.M. Meng, X.C. Zhu, X.H. Sun, Pore structure typing and fractal characteristics of lacustrine shale from Kongdian Formation in East China, J. Nat. Gas Sci. Eng., 85 (2021) 103709, doi: 10.1016/j.jngse.2020.103709.
[24] J.C. Qiao, J.H. Zeng, S. Jiang, Y.C. Zhang, S. Feng, X. Feng, H.T. Hu, Insights into the pore structure and implications for fluid flow capacity of tight gas sandstone: a case study in the upper paleozoic of the Ordos Basin, Mar. Pet. Geol., 118 (2020) 104439, doi: 10.1016/j.marpetgeo.2020.104439.
[25] T. Qu, Z.L. Huang, J.L. Chen, T.J. Li, J. Dong, Z.Y. Li, B. Wang, Y.Z. Yang, X.B. Guo, Pore structure characteristics and their diagenetic influence: a case study of paleogene sandstones from the Pinghu and Huagang Formations in the Xihu Depression, East China Sea Basin, Math. Geosci., 54 (2022) 1371–1412.
[26] R. Qiang, H. Wei, G.F. Lei, W.G. Zhang, B.Y. Ge, J.X. Nan, Effect of microscopic pore throat structure on displacement characteristics of lacustrine low permeability sandstone: a case study of Chang 6 reservoir in Wuqi Oilfield, Ordos Basin, Geofluids, 2022 (2022) 7438074, doi: 10.1155/2022/7438074.
[27] Q. Tong, D.B. He, Z.H. Xia, J.X. Huang, K.X. Di, F. Xu, S.W. Guo, Influence of reservoir pore-throat structure heterogeneity on water-flooding seepage: a case study of Yanchang Formation in Ordos Basin, Minerals, 12 (2022) 1243, doi: 10.3390/min12101243.
[28] S.T. Wu, R.K. Zhu, Z. Yang, Z.G. Mao, J.W. Cui, X.X. Zhang, Distribution and characteristics of lacustrine tight oil reservoirs in China, J. Asian Earth Sci., 178 (2018) 20–36.
[29] Y.Q. Xu, L.Y. Liu, Y. Zhu, Characteristics of movable fluids in tight sandstone reservoir and its influencing factors: a case study of Chang 7 reservoir in the Southwestern of Ordos Basin, J. Pet. Explor. Prod. Technol., 11 (2021) 3493–3507.
[30] X.Y. Zhong, L.Y. Liu, H.M. Wang, Z.Y. Xu, H. Chen, X.W. Wang, Y.S. Zhu, Characteristics and origins of the modal pore throat structure in weakly cemented sandy conglomerate reservoirs, J. Pet. Sci. Eng., 208 (2021) 109470, doi: 10.1016/j.petrol.2021.109470.
[31] G.L. Li, Y.H. Guo, H.C. Wang, X.K. Yang, Y.D. Hou, S.Y. Ye, K.Z. Zhang, Mechanism affecting the pore differentiation characteristics of fine-grained tight sandstones: a case study of Permian Shanxi Formation in Ordos Basin, ACS Omega, 8 (2023) 9499–9510.
[32] B.B. Luan, B. Zhang, D.D. Wang, C. Deng, F. Wang, 2022. Quantitative evaluation of tight oil reservoirs in the Chang 8 Member of the Yanchang Formation in southern Ordos Basin, Front. Earth Sci., 10 (2022) 963316, doi: 10.3389/feart.2022.963316.
[33] Y.M. Pang, X.W. Guo, X.C. Chang, J.J. Zhang, J.Q. Zhou, L.X. Cai, Characteristics and classification of paleozoic tight reservoirs in the central uplift of the South Yellow Sea Basin, Energy Geosci., 3 (2021) 383–393.
[34] Z.H. Jiang, Z.Q. Mao, Y.J. Shi, D.X. Wang, Multifractal characteristics and classification of tight sandstone reservoirs: a case study from the Triassic Yanchang Formation, Ordos Basin, China, Energies, 11 (2018) 2242, doi: 10.3390/en11092242.
[35] J. Peng, H.D. Han, Q.S. Xia, B. Li, Evaluation of the pore structure of tight sandstone reservoirs based on multifractal analysis: a case study from the Kepingtage Formation in the Shuntuoguole uplift, Tarim Basin, NW China, J. Geophys. Eng., 15 (2018) 1122–1136.
[36] J. Lai, G.W. Wang, J.T. Cao, C.W. Xiao, S. Wang, X.J. Pang, Q.Q. Dai, Z.B. He, X.Q. Fan, L. Yang, Z.Q. Qin, Investigation of pore structure and petrophysical property in tight sandstones, Mar. Pet. Geol., 91 (2018) 179–189.
[37] J.J. Wang, S.H. Wu, Q.H. Guo, The occurrence characteristic and dominant controlling factors of movable fluids in tight oil reservoirs: a case study of the Triassic tight sandstone in Ordos Basin, China, Arabian J. Geosci., 14 (2021) 205.
[38] Z.Z. Tan, W.M. Wang, W.H. Li, S.F. Lu, T.H. He, Controlling factors and physical property cutoffs of the tight reservoir in the Liuhe Basin, Adv. Geo-Energ. Res., 1 (2017) 190–202.
[39] W.-x. Han, X.-c. Chang, S.-z. Tao, W.-w. Yang, J.-l. Yao, Anomalies and genetic mechanism of ethane carbon isotope in the Ordovician carbonate reservoirs in the Jingbian gas field, Ordos Basin, China, Carbonates Evaporites, 1 (2020) 190–202.
[40] Y. Lu, K.Y. Liu, Pore structure characterization of eocene low-permeability sandstones via fractal analysis and machine learning: an example from the Dongying Depression, Bohai Bay Basin, China, ACS Omega, 6 (2021) 11693–11710.
[41] Z.J. Xu, L.F. Liu, T.G. Wang, K.J. Wu, X.Y. Gao, W.C. Dou, F. Xiao, N. Zhang, X.P. Song, H.T. Ji, Application of fluid inclusions to the charging process of the lacustrine tight oil reservoir in the Triassic Yanchang Formation in the Ordos Basin, China, J. Pet. Sci. Eng., 149 (2017) 40–55.
[42] Z.Q. Yang, X.L. Tang, H.M. Xiao, F. Zhang, Z.X. Jiang, G. Liu, Water film thickness of tight reservoir in Fuyu oil layer of Cretaceous Quantou Formation in Songliao Basin and its influence on the lower limit of seepage, Mar. Pet. Geol., 139 (2022) 105592, doi: 10.1016/j.marpetgeo.2022.105592.
[43] Y. Li, A.P. Fan, R.C. Yang, Y.P. Sun, N. Lenhardt, Sedimentary facies control on sandstone reservoir properties: a case study from the Permian Shanxi Formation in the southern Ordos basin, central China, Mar. Pet. Geol., 129 (2021) 105083, doi: 10.1016/j.marpetgeo.2021.105083.
[44] H.H. Liu, S.X. Sang, J.H. Xue, G.X. Wang, H.J. Xu, B. Ren, C.J. Liu, S.Q. Liu, Characteristics of an *in-situ* stress field and its control on coal fractures and coal permeability in the Gucheng block, southern Qinshui Basin, China, J. Nat. Gas Sci. Eng., 36 (2016) 1130–1139.
[45] J. Peng, H.D. Han, Q.S. Xia, B. Li, Fractal characteristic of microscopic pore structure of tight sandstone reservoirs in Kalpintag Formation in Shuntuoguole area, Tarim Basin, Pet. Res., 5 (2020) 1–17.
[46] P. Li, W. Sun, Y. Jian, R. Huang, H.X. Huang, Microscopic pore structure of Chang 63 reservoir in Huaqing oilfield, Ordos Basin, China and its effect on water flooding characteristics, J. Pet. Explor. Prod. Technol., 8 (2018) 1099–1112.
[47] M. Ali, W. Bian, K. Yang, S.K.P. Muhammad, Pore structures and reservoir characteristics of volcanic rocks in the Carboniferous Batamayineishan Formation in Shuangjingzi area, eastern Junggar Basin, Rud-Geol-Naft Zb., 36 (2021) 105–119.
[48] S.L. Li, Y.Z. Ma, X.H. Yu, S.L. Li, Reservoir potential of deep-water lacustrine delta-front sandstones in the Upper Triassic Yanchang Formation, Western Ordos Basin, China, J. Pet. Geol., 40 (2017) 105–118.
[49] W. Yang, Q.Y. Wang, Y.H. Wang, Z.X. Jiang, Y. Song, Y.H. Li, D. Liu, R. Zuo, X.M. Gu, F. Zhang, Pore characteristic responses to categories of depositional microfacies of delta-lacustrine tight reservoirs in the Upper Triassic Yanchang Formation, Ordos Basin, NW China, Mar. Pet. Geol., 118 (2020) 104423, doi: 10.1016/j.marpetgeo.2020.104423.

[50] K. Wu, D.Z. Chen, W.G. Zhang, H. Yang, H.N. Wu, X. Cheng, Y.Q. Qu, M.Q. He, Movable fluid distribution characteristics and microscopic mechanism of tight reservoir in Yanchang Formation, Ordos Basin, Front. Earth Sci., 10 (2022) 840875, doi: 10.3389/feart.2022.840875.
[51] J.Y. Zhang, S.Z. Tao, S.T. Wu, G.D. Liu, W.Z. Zhao, G.H. Li, Controlling effect of pore-throat structures on tight oil accumulation effectiveness in the upper Cretaceous Qingshankou formation, Songliao Basin, Geoenergy Sci. Eng., 225 (2023) 211689, doi: 10.1016/j.geoen.2023.211689.
[52] C.-N. Zou, Z. Yang, L.-H. Hou, R.-K. Zhu, J.-W. Cui, S.-T. Wu, S.-H. Lin, Q.-L. Guo, S.-J. Wang, D.-H. Li, Geological characteristics and "sweet area" evaluation for tight oil, Pet. Sci., 12 (2015) 606–617.
[53] P. Li, W. Sun, B.L. Wu, Y.L. Gao, K. Du, Occurrence characteristics and influential factors of movable fluids in pores with different structures of Chang 6_3 reservoir, Huaqing Oilfield, Ordos Basin, China, Mar. Pet. Geol., 97 (2018) 480–492.